The non-interacting hard-square lattice gas: Ising universality

1993 J. Phys. A: Math. Gen. 26 6679

(http://iopscience.iop.org/0305-4470/26/23/017)

J. Phys. A: Math. Gen. 26 (1993) 6679–6689. Printed in the UK

The non-interacting hard-square lattice gas: Ising universality

G Kamieniarz†‡§ and H W J Blöte†

† Faculty of Applied Physics, Delft University of Technology, Lorentzweg 1, 2628 CJ Delft, The Netherlands and ‡ Institute of Theoretical Physics, University of Leuven, Celestijnenlaan 200D, Leuven, Belgium

Received 21 December 1992

Abstract. The critical exponents of the non-interacting hard-square lattice gas model are determined by means of series analysis and finite-size scaling. The series analysis leads to results for the exponents that are consistent with the expected Ising universal values. A scaling analysis is performed on different types of numerical finite-size data obtained by means of the transfer-matrix method. The results support Ising universality. A procedure based on conformal invariance reproduces the known Ising temperature and magnetic exponents within 10^{-6}. Furthermore we estimate the critical density of the hard-square model as $\rho_c = 0.367\,743\,000\,(5)$.

1. Introduction

The commonly accepted notion of universality implies that critical points at the end of a two-phase coexistence line are Ising-like. Indeed, exact results and most results obtained from accurate numerical techniques support this point of view. A notable exception here is the series analysis by Baxter *et al* [1] of the non-interacting hard-square model. The size of the squares is such that they cannot sit on nearest-neighbour positions, but the squares do not interact otherwise. The absence or presence of a lattice-gas particle at site i is expressed by a variable $\sigma_i = 0$ or $\sigma_i = 1$, respectively. Denoting the activity of the gas particles as z, the partition sum is

$$Z = \sum_{\{\sigma_i\}} z^{\Sigma_i \sigma_i} \prod_{\langle i,j \rangle} (1 - \sigma_i \sigma_j). \tag{1}$$

The product is over all pairs of nearest-neighbour sites, and guarantees that configurations with interpenetrating particles do not contribute to Z.

The maximum particle density occurs when the squares occupy one of the two checkerboard-like sublattices. When the density of the squares is sufficiently lowered, a phase transition occurs to a disordered state in which the two sublattices are equally occupied. In the absence of an exact solution, Baxter *et al* [1] applied series expansion techniques to determine the critical exponents of this model. They found that the specific heat exponent at this critical point was $\alpha' = 0.09 \pm 0.05$, somewhat different from the exactly known value of the two-dimensional Ising model $\alpha' = 0$. However,

§ Permanent address: Institute of Physics, A. Mickiewicz University, Poznań, Poland.

0305-4470/93/236679+11 $07.50

subsequent analyses of the finite-size-scaling behaviour of the temperature derivative of the correlation length by Goldfinch and Wood [2] and by Racz [3] did not show significant deviations from Ising universality. Using scaling assumptions, one can express their results in terms of α'; then it appears that α' does not differ from zero by more than 2×10^{-2} [2] or 4×10^{-3} [3].

Thus, the evidence against the validity of Ising universality for the hard-square model is not convincing. Still, we found the result by Baxter *et al* sufficiently interesting to start some new work on this model. We expected that we might thus be able to find more compelling numerical evidence that the hard-square model is inside the Ising universality class, or perhaps to demonstrate deviations from Ising universality more clearly.

A possibility to obtain very accurate results is by means of transfer-matrix techniques and finite-size scaling [4], as demonstrated, for example, in a recent analysis by Blöte and Wu [5] of the square-lattice antiferromagnetic Ising model in a magnetic field. The non-interacting hard-square model is a special case of this model: it is obtained in the limit of an infinitely strong field. The availability of an accurate result for the critical point of the hard-square model may already be a sufficient reason to re-analyse the series of Baxter *et al* [1]. That will be the subject of section 2. Our results do not show convincing deviations from the expected Ising universal behaviour. Furthermore, we have made several finite-size scaling approaches to the problem, using different sets of scaling assumptions and system shapes. In section 3.1, we analyse transfer-matrix results for square systems with periodic boundaries. In section 3.2, we use instead cylindrically shaped systems that are infinitely long in one direction. The most accurate exponents thus obtained agree with Ising universality within a margin of 10^{-6}.

2. Analysis of the high-density series

The value of the critical activity where the translational symmetry of the model (1) is spontaneously broken is denoted z_c. A recent determination yielded [5]

$$z_c = 3.796\,255\,174\,(3) \tag{2}$$

(the uncertainty in the last decimal place is given in parentheses) corresponding to a chemical potential $\mu_c = 1.344\,015\,100\,4\,(8)$. This result was obtained with the transfer matrix method and using the assumption of Ising universality. Then the 'finite-size divergence' of the correlation length at the critical point is given by

$$\xi(L) \sim AL$$

where A is a universal amplitude (Blöte and Nightingale [6] and references therein). It has the value $4/\pi$ for the magnetic corrrelation function, and $1/(2\pi)$ for the energy-energy correlation function. Thus, the critical point and critical exponents can be estimated from finite-size data for the correlation length.

Here we emphasize that this assumption *does not bias the determination of the critical point*. The application of a wrong value of the amplitude in the finite-size analysis will influence the finite-size estimates of the critical point, but not their limit, as long as the temperature-like variable (chemical potential or activity) is relevant. Thus, the extrapolation procedure will still lead to the correct result.

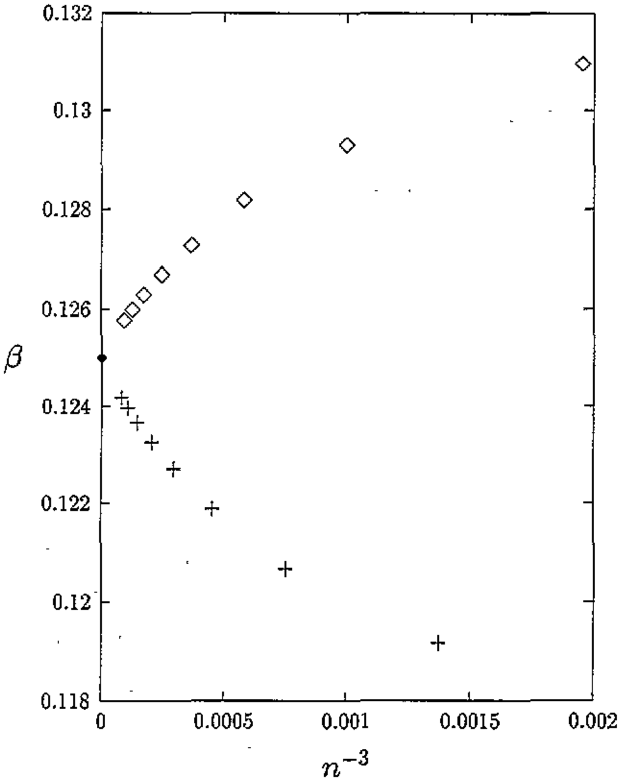

Figure 1. The behaviour of $\beta(r_n)$ as a function of n^{-3}. The data for even n are shown by ◇ and those for odd n by +. Iterated fits indicate that $\beta = 0.1249(1)$, in agreement with the expected Ising value $\frac{1}{8}$ (shown by •).

On the basis of the result (2) for the critical activity z_c, the series expansions of Baxter *et al* [1] can be re-analysed. Thus we consider expansion of the order parameter (i.e. the staggered density) R in terms of the inverse activity $x = 1/z$:

$$R^{-8}(x) = \sum_{n=0}^{\infty} R_n x^n. \tag{3}$$

The ratios $r_n = R_n/R_{n-1}$ asymptotically obey

$$r_n \simeq z_c\left[1 + \frac{1}{n}(8\beta - 1)\right]. \tag{4}$$

We have thus estimated the critical exponent β by solving (4) for β, using (2) and the coefficients R_n listed in table II of [1]. The solutions are denoted $\beta(r_n)$. On the basis of the mechanism of corrections-to-scaling, we expect that the $\beta(r_n)$ will converge to β with a power of n. Power-law fits indicate that the leading correction behaves approximately as n^{-3}, but additional corrections are prominent. Different amplitudes apply to even and odd n. This behaviour of $\beta(r_n)$ is shown in figure 1 versus n^{-3}. Iterated fits [6, 7] indicate that $\beta = 0.1249$ (1), in agreement with Ising universality.

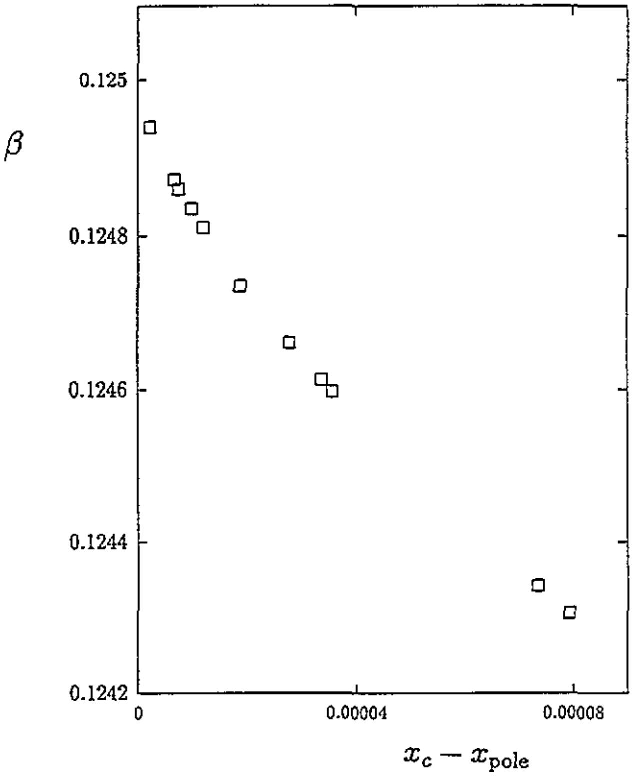

Figure 2. The residues of the D-log Padé approximants of the series $R(x)$ versus the *deviations of the corresponding poles from the critical value* x_c.

Next, we consider the D log Padé analysis of the series $R(x)$ presented in table I of [1]. We show the results for β in figure 2 as a function of the distance of the corresponding poles from the critical value $x_c = 1/z_c = 0.263\,417\,488$. The dependence of the residues of $(d/dx)\ln R(x)$ on this distance is remarkably smooth. These data indicate that β does not differ from 1/8 by more than a few times 10^{-5}.

Baxter *et al* [1] concluded that the staggered density series in ρ is not long enough to give reliable estimates of the exponents since ρ displays only a weak singularity. As a result of the D log Padé analysis of $R(\rho') \sim (\rho'_c - \rho)^{\beta/(1-\alpha')}$, where $\rho' = 1 - 2\rho$, and assuming $\beta = 1/8$, they found $\alpha' = 0.09 \pm 0.05$, somewhat different from the Ising value $\alpha = 0$. Alternatively, one can analyse a derivative of the series in which the singularity appears more strongly [8]. We chose the series

$$\rho^{(2)} \equiv \frac{d^2}{dx^2}\rho' \sim (x_c - x)^{-1-\alpha'} \tag{5}$$

which can be found from

$$\rho' = 1 - 2\rho = \sum_{n=1}^{\infty} \rho_n x^n \tag{6}$$

Table 1. The coefficients of the series $\rho'(x)$ and D log Padé approximants of the series $\rho^{(2)}$.

n	ρ_n	[N, D]	Pole	Residue
1	1	[6, 7]	0.265 262	1.110 4
2	−1			
3	4	[7, 6]	0.264 756	1.095 8
4	−9			
5	36	[7, 7]	0.264 651	1.092 6
6	−106			
7	407	[7, 8]	0.264 159	1.074 1
8	−1 281			
9	4 819	[8, 7]	0.264 822	1.097 2
10	−15 806			
11	59 280	[8, 8]	0.264 056	1.069 4
12	−200 046			
13	749 958	[8, 9]	0.264 289	1.078 6
14	−2 580 901			
15	9 677 199	[9, 8]	0.263 819	1.055 8
16	−33 777 265			
17	126 680 074	[9, 9]	0.263 368	1.019 3
18	−446 859 565			
19	1 676 434 924	[9, 10]	0.263 925	1.063 2
20	−5 962 612 074			
21	22 378 164 365	[10, 9]	0.263 708	1.0 484
22	−80 124 302 732			
23	300 839 190 930	[10, 10]	0.263 711	1.0 486

of which the coefficients are determined by those given in appendix B in [1]. In table 1 we list the coefficients ρ_n of the series $\rho'(x)$ as well as the poles and the residues of $(\mathrm{d}/\mathrm{d}x)\ln \rho^{(2)}$. These estimates of α' are plotted by diamonds in figure 3 as a function of $x_c - x_{\text{pole}}$. For comparison, the corresponding estimates of Baxter *et al.* [1] are given by squares versus $\rho'_c - \rho'_{\text{pole}}$, where $\rho'_c = 0.264\,514$ (see the finite-size scaling analysis in section 3). Both sets of data cover a smooth curve as a function of the deviation of the pole from the critical value. It appears that the results taken from table 1 fall much closer to 0.

In view of correction terms present, we are unaware of an *a priori* reason why the analysis of $\rho^{(2)}(x)$ should produce better results than that of $R(\rho')$. The data collapses in figure 3 are better than those in plots versus $1/(N+D)$ where $[N, D]$ indicates the degrees of the approximants. On the basis of such a plot for $(\mathrm{d}/\mathrm{d}x)\ln \rho^{(2)}$ series we estimate $\alpha' = -0.1$ (1). Thus the analysis of $\rho^{(2)}$ indicates that α' may be smaller than the result obtained from the $R(\rho')$ series [1].

3. Finite-size scaling analysis

We consider the model (1) on $L \times L$ and $L \times \infty$ square lattices with periodic boundary conditions. To enable the introduction of two sublattices in a checkerboard-like fashion, L is restricted to be even. We use the transfer matrix technique in order to calculate numerically the partition sum (1), as well as some of its derivatives.

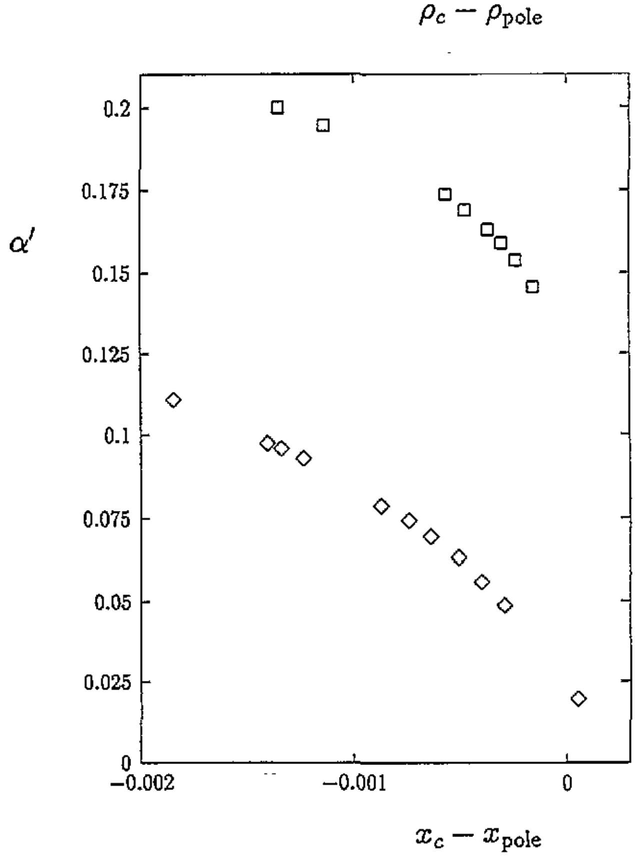

Figure 3. The dependence of the α' estimates found from the D-log Padé approximants on the deviations of the poles from the critical point. The present data are shown versus $x_c - x_{\text{pole}}$ by ◇, and those of Baxter *et al.* versus $\rho_c - \rho_{\text{pole}}$ by □.

Denoting the lattice gas variables $(\sigma_{j1}, \sigma_{j2}, \ldots, \sigma_{jL})$ in the jth row of the lattice by $\boldsymbol{\sigma}_j$, the elements of the row-to-row transfer matrix $\mathbf{T}$ are

$$T(\boldsymbol{\sigma}_i, \boldsymbol{\sigma}_j) = x^{(\mu/2)\Sigma_{k=1}^{L}(\sigma_{i,k}+\sigma_{j,k})} \prod_{k=1}^{L} (1-\sigma_{i,k}\sigma_{j,k})(1-\sigma_{i,k-1}\sigma_{i,k})(1-\sigma_{j,k-1}\sigma_{j,k}) \tag{7}$$

with $\sigma_{i,0} = \sigma_{i,L}$ in accordance with the periodic boundary conditions. The partition sum (1) of a system consisting of M rows is equal to

$$Z = \operatorname{Tr} \mathbf{T}^M. \tag{8}$$

For the numerical purpose of calculating Z, it is sufficient to have an algorithm available that computes the vector $\mathbf{T} \cdot \boldsymbol{v}$ from a given vector $\boldsymbol{v}$ with elements $v(\boldsymbol{\sigma})$. Since the transfer matrix can be decomposed in a product of sparse matrices, it is not necessary to store the whole matrix $\mathbf{T}$ in the computer memory [4]. In this way it is no problem to perform calculations up to about $L = 20$. For further details of the numerical methods, see [5–7, 9].

Table 2. Finite-size data for square systems for $2\rho_L$, c_L and χ_L.

L	$2\rho_L$	c_L	χ_L
2	0.809 089 805 642 114 0	0.140 234 999 156 698 9	0.724 743 813 172 343
4	0.774 971 280 168 877 7	0.192 247 445 951 476 7	2.447 647 203 710 980
6	0.761 672 521 630 242 5	0.224 600 286 587 782 2	4.978 297 322 277 479
8	0.755 063 942 755 142 6	0.247 705 748 541 591 2	8.241 664 994 051 973
10	0.751 121 421 754 400 6	0.265 657 038 171 807 4	12.186 091 898 838 77
12	0.748 502 156 061 453 1	0.280 325 299 243 233 8	16.773 814 255 597 46
14	0.746 635 359 180 546 2	0.292 721 963 182 031 0	21.975 681 723 236 16
16	0.745 237 325 668 847 3	0.303 454 575 700 854 5	27.768 176 645 488 04

3.1. Square systems

The perturbation scheme described in [10, 9] is used to compute the first and second derivatives $Z^{(1)}$ and $Z^{(2)}$ of the partition sum (8) with respect to the chemical potential μ of the lattice gas particles. This method yields more accurate results than numerical differentiation. In the present application of the scheme, the infinite nearest-neighbour repulsion K_∞ plays the role of K_x and K_y in [9], and $\Delta\mu = \mu - \mu_c$ that of the field h.

The first derivative determines the lattice gas density $\rho_L = Z^{(1)}/L^2 Z$, and the second one the specific heat $c_L = Z^{(2)}/L^2 Z - (Z^{(1)}/LZ)^2$. The finite-size quantities ρ_L and c_L for $L \times L$ systems are given in table 2 for L up to 16.

To improve the convergence of the finite-size estimates of the critical density ρ_c', and anticipating the outcome of the present analysis, we make use of the assumption that the model (1) belongs to the $d=2$ Ising universality class. Thus we expect that the density ρ_L scales as the energy [11, 12, 9]:

$$\rho_L = \rho_c + a_1 L^{-1} \ln L + a_2 L^{-1} + a_3 L^{-2} + \cdots . \tag{9}$$

Iterated power-law fits [6, 7] in accordance with (9) yield the result

$$\rho_c/\rho_{\max} = 0.735\,49\,(2) \tag{10}$$

with $\rho_{\max} = \frac{1}{2}$. Note that, even if the exponents of L in (9) were incorrect (i.e. the model would not obey Ising universality), the fitting procedure would still converge to the correct result with increasing system sizes.

For the determination of the temperature exponent from the density data, we use the asymptotic finite-size scaling formula

$$\rho_L \simeq \rho_c + L^{y_t - d}(a_1 + a_2 L^{-p}) \tag{11}$$

where $d=2$ is the dimensionality, and the term with exponent $-p$ represents a correction to scaling. Adopting the value of ρ_c found above, the fitting procedure yields

$$y_t = 1.000\,(2). \tag{12}$$

The finite-size scaling dependence of the specific heat is

$$c_L \simeq L^{2y_t - d}(b_1 + b_2 L^{-q}) \tag{13}$$

so that fits applied to the c_L data allow another estimate of the temperature exponent. We obtain

$$y_t = 1.000\,(6). \tag{14}$$

Another exponent of interest is the magnetic exponent y_h. It may be determined from the finite-size dependence of the staggered susceptibility. Thus we introduce a staggered field h acting with different signs on the two sublattices, i.e. a term $(-)^{i+j}h$ in the reduced Hamiltonian per spin with coordinates (i, j). The inclusion of such a term in the transfer matrix is quite straightforward. The second derivative of Z to h yields the staggered susceptibility χ_L. Numerical data at the critical point are obtained from a perturbation expansion of Z in h, quite analogously to the calculation of c_L. We skip the technical details, except the remark that one has to distinguish between the even and odd rows of the lattice during the calculation, because the staggered field changes sign. The finite-size data for χ_L are included in table 2. They are expected to scale as

$$\chi_L \simeq L^{2y_h-d}(c_1+c_2L^{-r}). \tag{15}$$

The fits and power-law extrapolations then yield the result

$$y_h = 1.875\,00\,(5). \tag{16}$$

3.2. Infinitely long systems

In the limit $M \to \infty$, the partition sum (8) satisfies

$$\lim_{M\to\infty} Z^{1/M} = \lambda_0 \tag{17}$$

where λ_0 is the largest eigenvalue of $\mathbf{T}$. Denoting the corresponding eigenvector by $\boldsymbol{v}_0$, and differentiating the free energy per site $f = \log Z^{1/LM}$ to μ leads to

$$\rho_L = \frac{1}{L}\frac{\mathrm{d}}{\mathrm{d}\mu}\log\frac{\boldsymbol{v}_0\cdot\mathbf{T}\cdot\boldsymbol{v}_0}{\boldsymbol{v}_0\cdot\boldsymbol{v}_0}. \tag{18}$$

Both $\boldsymbol{v}_0$ and $\mathbf{T}$ depend on μ in first order. However, since $\mathbf{T}$ is symmetric, the first-order contribution to Z due to $\boldsymbol{v}_0$ vanishes. Therefore,

$$\rho_L = \frac{1}{L}\frac{\boldsymbol{v}_0\cdot\mathbf{T}'\cdot\boldsymbol{v}_0}{\boldsymbol{v}_0\cdot\mathbf{T}\cdot\boldsymbol{v}_0} = \frac{1}{L}\frac{\boldsymbol{v}_0\cdot S\cdot\boldsymbol{v}_0}{\boldsymbol{v}_0\cdot\boldsymbol{v}_0} \tag{19}$$

where $\mathbf{T}' = \mathrm{d}T/\mathrm{d}\mu$ and S is diagonal with elements

$$S(\boldsymbol{\sigma}_i, \boldsymbol{\sigma}_j) = \delta_{\sigma_i,\sigma_j}\sum_{k=1}^{L}\sigma_{i,k} \tag{20}$$

so that $\mathbf{T}' = \frac{1}{2}(\mathbf{S}\cdot\mathbf{T}+\mathbf{T}\cdot\mathbf{S})$. The eigenvector, which can numerically be determined by the conjugate-gradient method [13], thus determines the density ρ_L. Finite-size data up to $L=20$ are presented in table 3. These data indicate that the second and third term on the right-hand side of (9) are absent for these elongated systems. The largest occurring power of L appears to be about -4. Iterated fits accounting for such a correction term yield

$$\rho_c/\rho_{\max} = 0.735\,486\,00\,(1). \tag{21}$$

The next-largest eigenvalues of T are associated with the exponential decay of correlation functions. The inverse correlation lengths are equal to the 'gaps' $g_i(L)$ in the eigenvalue spectrum:

$$g_i(L) = \xi_i^{-1}(L) = \log\frac{\lambda_0}{|\lambda_i|}. \tag{22}$$

Table 3. Finite-size data for infinitely long systems.

L	$2\rho_L$	$g'_m(L)$	$2\pi g_m(L)$	$2\pi g_t(L)$
2	0.726 244 058 108 471	−0.273 755 941 891 529	0.117 312 343 954 852	∞
4	0.734 551 521 141 716	−0.257 141 015 883 448	0.122 897 437 477 144	1.492 501 752 647 339
6	0.735 264 781 185 881	−0.253 123 074 668 091	0.124 046 855 005 525	1.121 420 005 335 352
8	0.735 408 617 687 668	−0.251 763 787 044 615	0.124 464 412 999 446	1.060 768 848 639 344
10	0.735 452 218 732 831	−0.251 169 009 236 913	0.124 659 218 713 833	1.037 092 738 295 593
12	0.735 468 961 546 115	−0.250 862 019 414 078	0.124 764 844 822 631	1.025 140 640 628 718
14	0.735 476 484 295 798	−0.250 684 793 622 105	0.124 828 232 680 120	1.018 210 205 128 867
16	0.735 480 267 636 423	−0.250 573 910 761 620	0.124 869 154 362 282	1.013 816 616 102 912
18	0.735 482 339 629 123	−0.250 500 208 376 032	0.124 897 065 375 393	1.010 850 140 618 826
20	0.735 483 551 262 701	−0.250 448 876 309 532	0.124 916 935 356 005	1.008 750 497 149 675

The magnetic correlation length corresponds with the eigenvalue λ_1 that is second largest in absolute value. In accordance with the alternating behaviour of the magnetic correlations, this eigenvalue is negative. It can, together with the corresponding eigenvector v_1, simply be obtained by application of the conjugate-gradient method [13] to the negative side of the eigenvalue spectrum. Differentiation of the magnetic gap to μ leads, in analogy with (19), to

$$g'_l(L)=\frac{d\xi_1^{-1}(L)}{d\mu}=\frac{v_0\cdot\mathbf{S}\cdot v_0}{v_0\cdot v_0}-\frac{v_1\cdot\mathbf{S}\cdot v_1}{v_1\cdot v_1} \tag{23}$$

Numerical data for $g'_l(L)$ are included in table 3. Finite-size scaling predicts that

$$g'_l(L)\simeq L^{y_l-1}(u+vL^{-w}). \tag{24}$$

Fitting an expression of this form to the data, and subsequent iterated fits lead to the result

$$y_t=1.000\,01\ (2). \tag{25}$$

Another way to determine critical exponents uses conformal invariance. A relation derived by Cardy [14] applies to the finite-size amplitude of the correlation lengths:

$$\lim_{L\to\infty} L/\xi_i=2\pi x_i \tag{26}$$

where $x_i=d-y_i$ is the anomalous dimension of the observable associated with the correlation length ξ_i. Thus the sealed gaps $Lg_i(L)/(2\pi)$ provide estimates of x_i. Numerical data for the scaled magnetic gap are presented in table 3. Power-law extrapolation yields

$$y_h=1.875\,000\ (1). \tag{27}$$

A similar determination was done for the temperature exponent. The energy–energy correlation function is associated with the eigenvalue λ_2 that is third largest in absolute value. It is positive (and hence the second largest). The associated eigenvector v_2 has the same symmetry properties as the leading eigenvector (invariant under translations in the finite direction of the lattice). It may be obtained by means of the conjugate-gradient algorithm using orthogonalization with respect to the leading eigenvector.

Finite-size results for the resulting scaled gaps $Lg_2(L)/(2\pi)$ are shown in table 3. Subsequent power-law extrapolation yields

$$y_t = 1.000\,000\,(1). \tag{28}$$

4. Discussion

In order to shed more light on the problem concerning the universal classification of the non-interacting hard-square model, we have determined its critical exponents using a variety of methods with different scaling assumptions. The series analysis of the density as a function of the inverse activity was analysed using Padé approximants, and yielded a specific-heat exponent considerably closer to the Ising value 0 than the result found by Baxter *et al* [1] from the staggered density series as a function of the density.

We see no *a priori* reason for which of the series results for α should be the more accurate one. We interpret the difference as a confirmation that the series containing ρ are too short for a reliable determination of the critical exponents. It seems reasonable to conclude that the numerical results of the series analyses are, although not very accurate, consistent with Ising universality.

The assumptions involved in the finite-size analysis amount to the analyticity of renormalization transformations employing an additional finite-size field [15] $1/L$ with exponent $y_L = 1$. Thus, the analysis will yield results in terms of the renormalization exponents y_h and y_t. Other exponents follow from these by means of scaling. Here the main interest is in the value of y_t in view its relevance for the specific heat exponent $\alpha = (d - y_t)/y_t$.

We have determined finite-size data for several quantities: the density of the lattice gas particles, the specific heat, the staggered susceptibility, and the temperature derivative of the magnetic correlation length. The scaling behaviour of all these data is in an accurate agreement with the Ising universal exponents.

Another approach intimately related with renormalization was made using the hypothesis of conformal invariance. The temperature and magnetic exponents were determined using the relation between exponents and the finite-size amplitude of the associated correlation lengths. The results are in precise agreement (within one millionth) with the exactly known Ising values $y_h = 15/8$ and $y_t = 1$.

In addition to these results for the exponents, we mention that a recent determination [9] of the universal amplitude ratio $Q = \langle R^2\rangle^2/\langle R^4\rangle$ defined on the distribution of the order parameter R of the critical hard-square model yielded $Q = 0.856\,25\,(5)$, in agreement with the accurately known Ising value [9].

Summarizing, the whole body of available numerical results provides strong evidence that the non-interacting hard-square model belongs to the Ising universality class, in agreement with the topology of the phase diagram.

Acknowledgments

It is a pleasure to thank Y T J C Fonk, H J M van Grol, J R Heringa and Y M M Knops for many valuable discussions.

References

[1] Baxter R J, Enting I G and Tsang S K 1980 *J. Stat. Phys.* **22** 465
[2] Wood D W and Goldfinch M 1980 *J. Phys. A: Math. Gen.* **13** 2781
[3] Racz Z 1980 *Phys. Rev. B* **21** 4012
[4] Nightingale M P 1975 *Phys. Lett.* **59A** 486; 1976 *Physica* **A83** 561; 1979 *Proc. Kon. Ak. Wet. B* **82** 235
[5] Blöte H W J and Wu X N 1990 *J. Phys. A: Math. Gen.* **23** L627
[6] Blöte H W J and Nightingale M P 1983 *J. Phys. A: Math. Gen.* **16** L657
[7] Blöte H W J, Wu F Y and Wu X N 1990 *Int. J. Mod. Phys.* B **4** 619
[8] Fisher M E and Au-Yang H 1979 *J. Phys. A: Math. Gen.* **12** 1677
[9] Kamieniarz G and Blöte H W J 1993 *J. Phys. A: Math. Gen.* **25** 201
[10] Saleur H and Derrida B 1985 *J. Physique* **46** 1043
[11] Aharony A and Fisher M E 1983 *Phys. Rev.* B **27** 4394
[12] Privman V and Fisher M E 1984 *Phys. Rev.* B **30** 322
[13] Bradbury W W and Fletcher R 1969 *Num. Math.* **9** 259;
Press W H, Flannery B P, Teukolsky S A and Vetterling W T 1986 *Numerical Recipes* (Cambridge, Cambridge University Press)
[14] Cardy J L 1984 *J. Phys. A: Math. Gen.* **17** L385
[15] Suzuki M 1977 *Progr. Theor. Phys.* **58** 1142